timum values of the parameters of this equation to fit the conductance kinetic data, i.e., the values of $[HX]_i$ and t_i. Because of interdependencies, all five parameters k_1, k_2, k_3, t_0, and $[HX]_\infty$ could not be accurately determined simultaneously; therefore, calculations were done with fixed values assigned for either one or both of k_2 and k_3. The program can also be used to calculate first-order rate coefficients where the parameters are k_3, t_0, and $[HX]_\infty$ with k_1 and k_2 set to 0.

It was determined from calculations on synthetic data generated with probable values of k_1, k_2, k_3, t_0, and $[HX]_\infty$ that, when k_3 is small but kinetically significant, setting k_2 to its true value and k_3 to 0 will result in a small systematic wave in the plot of the resistance residuals. Error plots with such systematic trends were observed for **2b** in 80E and 90E, see Figure 4 in the supplementary material. The fit of the data from **2b** in 95E as described above produced a wave in the opposite sense which was shown to be due to the presence of a fraction of 1% pemsyl chloride impurity. These data were analyzed using a Simplex algorithm, which had been developed previously in our laboratory.[48] It was applied in this case to fit conductance data from the solvolysis of a mixture of two components: the ester **2b** reacting according to the kinetic scheme described above and the chloride reacting by a simple first-order process. The number of variables derived from the least-squares treatment was reduced to four by fixing k_2 and the solvolysis rate constant for pemsyl chloride at the independently observed values and constraining k_3 by fixing f_{rel} at 0.968, the value found to give optimum fits to all kinetic runs.

Supplementary Material Available: Figures 3, 4, and 5, showing the trends in the errors in the calculated resistances ("resistance residuals") over the time span of the solvolysis of **2a** and **3b** in 90E and **2b** in 80E using the simple first-order rate law and the rate law given in the Appendix for Scheme I (4 pages). Ordering information is given on any current masthead page.

Ultrathin Monolayer Lipid Membranes from a New Family of Crown Ether-Based Bola-Amphiphiles

Servando Muñoz, Jesus Mallén, Akio Nakano, Zhihong Chen, Isabelle Gay, Luis Echegoyen, and George W. Gokel*

Contribution from the Department of Chemistry, University of Miami, Coral Gables, Florida 33124. *Received April 23, 1992. Revised Manuscript Received October 23, 1992*

Abstract: Twelve novel α,Ω-bis(*N*-azacrown ether) compounds have been prepared, characterized, and converted into a previously unknown type of niosome. Four are bis(15-crown-5) derivatives having the following spacer chains: $(CH_2)_{12}$ (**1**), $(CH_2)_{16}$ (**2**), $CO(CH_2)_{20}CO$ (**3**), and $(CH_2)_{22}$ (**4**). The eight bis(aza-18-crown-6) derivatives have the following spacers: $(CH_2)_{10}$ (**5**), $CO(CH_2)_{10}CO$ (**6**), $(CH_2)_{12}$ (**7**), $CO(CH_2)_{14}CO$ (**8**), $(CH_2)_{16}$ (**9**), $(CH_2)_{22}$ (**10**), $(CH_2)_{12}O(CH_2)_{12}$ (**11**), and $CO(CH_2)_{11}S(CH_2)_{12}S(CH_2)_{11}CO$ (**12**). Aggregation studies of **1** and **7**, employing transmission electron microscopy as well as dynamic and static light scattering, demonstrate that these compounds form a novel class of spherical monolayer lipid membrane vesicles when dispersed in water. Debye light-scattering profiles obtained from a suspension of large (≈200 nm diameter) vesicles indicate a relative refractive index near 1. Dynamic turbidimetry in acidic media on a suspension of bola-amphisomes formed from **1**, suggested that the contribution of micelle–vesicle equilibria to the bolyte aggregation state is negligible. In neutral or slightly alkaline pH at 35 °C, the vesicles grew irreversibly to yield large, probably multilamellar, aggregates. In acidic media at pH 2, the bola-amphisomes do not coalesce, even at 65 °C. On the basis of the observations presented here, bola-amphiphiles having a hydrocarbon span of 10–12 carbon atoms aggregate in aqueous media into vesicles. When the aliphatic backbone incorporates 16 or more carbon atoms, micelles are formed.

Introduction

Nearly a decade ago, Fuhrhop and co-workers reported the synthesis and self-assembly properties of several hydrophobic derivatives of succinic acid in which two polar headgroups are linked covalently by a hydrophobic, saturated hydrocarbon skeleton (Figure 1).[1] Fuhrhop called these surfactant molecules bola-amphiphiles—the name derives from the South American slingshot comprised of two leather balls attached to a string. Bolas are designed to tangle around the legs of cattle and thereby immobilize them. Their molecular counterparts (bola-amphiphiles) often remain extended when dispersed in water and form monolayer lipid membrane vesicles or *bola-amphisomes*.

The covalent chains of bola-amphisome monomers need not interdigitate in the bilayer midplane as do normal amphiphiles. A covalent span of 12 carbons affords an "ultrathin" membrane with a width of less than 20 Å compared to common biological bilayer membranes that have thicknesses ranging from about 30 to 100 Å.[2] The monomers normally involved in the formation of bilayer membranes interdigitate along the membrane's midplane.[3] When the extent of interlaminar overlap becomes small, some of the surfactant monomers protrude from the membrane and are readily exchanged by intercolloidal collisions.[4,5] This process facilitates coalescence of the vesicles to yield larger, heterogeneous, multilamellar assemblies. In the case of a covalently linked monolayer membrane, the frequency of intervesicular fusion is reduced because both vertical diffusion and intervesicular exchange of surfactant monomers are inhibited.

Covalently linked dipolar surfactants are found in the membrane of thermophilic archaebacteria (unicellular organisms that live in boiling water under conditions of high ionic strength and low pH[6]). Such bacteria maintain an intracellular pH of about 6.5 when the external pH is 1.5. Gliozzi et al.[7] isolated from the

(1) Fuhrhop, J.-H.; Bach, R. In *Advances in Supramolecular Chemistry*; Gokel, G. W., Ed; Vol. 2, JAI Press: Greenwich, CT, 1992; Vol. 2, pp 25–63.
(2) Yeagle, P. *The Membranes of Cells*; Academic Press: New York, 1987.
(3) Kim, J. T.; Mattai, J.; Shipley, G. G. *Biochemistry* **1987**, *26*, 6592.
(4) Fendler, J. H. *Membrane Mimetic Chemistry*; J. Wiley and Sons: New York, 1982.
(5) Guillaume, B. C. R.; Yogev, D.; Fendler, J. H. *J. Phys. Chem.* **1991**, *95*, 7489.
(6) (a) Gliozzi, A.; Paoli, G.; Rolandi, R.; de Rosa, R.; Gambacorta, A. *J. Electroanal. Chem.* **1982**, *141*, 591.
(7) Gliozzi, A.; Rolandi, R.; de Rosa, M.; Gambacorta, A. *J. Membrane Biol.* **1983**, *75*, 45.

0002-7863/93/1515-1705$04.00/0

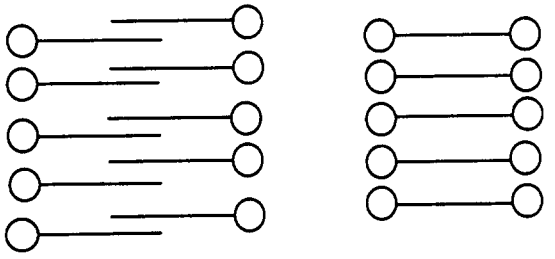

Figure 1. Bilayer (left) and monolayer lipid membranes.

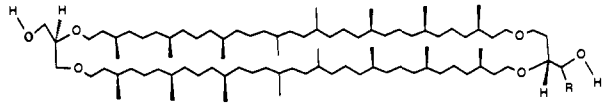

Figure 2. Archaebacteria membrane.

membrane of *Caldariella acidophila* the bola-amphiphathic surfactant shown in Figure 2. They noted that the survival of these bacteria depends in part on the strength of their monolayer cell walls: the covalent link between the polar headgroups precludes vertical dissociation of the membrane, while weak intermonomeric van der Waals attractive forces inhibit lateral lysis. The headgroups probably strengthen the membrane against both transversal and longitudinal lysis because of their contribution to the formation of intermonomeric, hydrogen-bonded domains.

Because of their ability to withstand physicochemical stress, monolayer membranes may be useful in such applications as the construction of molecular energy transducers and energy storage devices and perhaps in drug delivery applications. The latter is related to our development of redox-switched vesicles based on the ferrocene nucleus.[8] Indeed, we have extensive experience in the formation of crown-based membrane systems.[9] We now report the synthesis of 13 novel bola-amphiphiles and present a detailed study of the first bola-amphisome formation from such crown ether-based structures.

Results and Discussion

Syntheses. The bola-amphiphile compounds reported in this paper are *N*-substituted derivatives either of aza-15-crown-5 or aza-18-crown-6. The nitrogen atoms of the crown ethers are spanned by a variety of spacer units such as dodecane (-$(CH_2)_{12}$-) and hexadecanedioyl (-$CO(CH_2)_{14}CO$-), making all of the bola-amphiphiles either bis(tertiary amines) or bis(amides). Among these, the aggregation behavior of compounds **1** and **7** was studied most thoroughly. 1,12-Bis(aza-15-crown-5)dodecane (**1**) and 1,12-bis(aza-18-crown-6)dodecane (**7**) were prepared from the dodecanedioic acid and the appropriate crown[10] by acylation by dodecanedioyl chloride of either aza-15-crown-5 or aza-18-crown-6, followed by lithium aluminum hydride reduction of the amide. The double acylation was effected in 70% yield in both cases, and reduction afforded 76% of **1** and 72% of **7**. The sequence and structures are shown in Scheme I. The oily products were purified by chromatography and were fully characterized. Compounds **1**–**12** are shown in Table I.

Aqueous Self-Assembly. Bola-amphiphiles **1**, **5**, and **7** aggregate in aqueous media to yield vesicles (Table I). The compounds contain 10–12-carbon backbone spans that are terminated by aza-15-crown-5 or aza-18-crown-6. The diamidic precursor **6** to

Scheme I

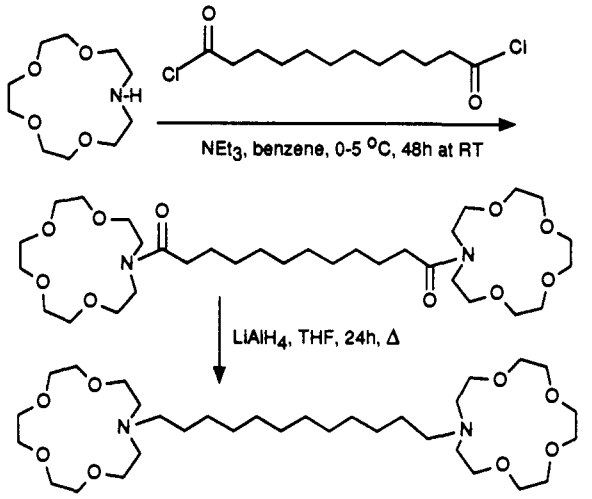

Table I. Novel Bis(crown) Bola-Amphiphiles

compd no.	ring size	spacer chain	yield (%)	mp (°C)	aggn state[a]
1	15	$(CH_2)_{12}$	76	oil	vesicle
2	15	$(CH_2)_{16}$	78	65–66	micelle
3	15	$CO(CH_2)_{20}CO$	69	76–78	micelle
4	15	$(CH_2)_{22}$	73	55–56	micelle
5	18	$(CH_2)_{10}$	45	oil	vesicle
6	18	$CO(CH_2)_{10}CO$	79	oil	micelle
7	18	$(CH_2)_{12}$	72	oil	vesicle
8	18	$CO(CH_2)_{14}CO$	72	oil	micelle
9	18	$(CH_2)_{16}$	70	48–49	micelle
10	18	$(CH_2)_{22}$	71	58–59	micelle
11	18	$(CH_2)_{12}O(CH_2)_{12}$	61	oil	micelle
12	18	$CO(CH_2)_{11}S(CH_2)_{12}$-$S(CH_2)_{11}CO$	57	wax	vesicle

[a] Determined by dynamic light scattering and/or transmission electron microscopy.

Table II. Aggregation Properties of Bola-Amphiphilic Derivatives of Crown Ethers at 25 °C[a]

	diameter, Å[b]	
compd no.	dynamic turbidimetry	transmission electron microscopy
1	730	760
7	1200	1180

[a] 2–5 mM bolyte in water, dispersed for 30 min at 10 °C, using an ultrasonic cell disruptor equipped with a titanium microtip and operated at 40 W. [b] The uncertainty in the measured diameter is ±30%.

7 forms micelles. Likewise, diamides **3**, **6**, and **8** form micelles. This suggests that all diamidic bola-amphiphiles may do so. Compound **12** is an exception to this possible generalization, but we feel that compound **12** is a special case because it contains a chain that is overall far longer than any other compound and it includes two heteroatoms. Otherwise, those compounds having backbones containing 16 carbon atoms or more appear to favor micelle formation. This suggests that as the length of the spine increases, the surfactant monomers become folded about the midplane of the covalent span forming structures that favor micelles.

When the 1,12-bis(aza-15-crown-5)dodecane bola-amphiphile **1** was dispersed in water by ultrasonic irradiation at 10 °C, an almost optically transparent suspension of aggregates was formed. The hydrodynamic diameters of these particles measured by dynamic turbidimetry is about 730 Å (Table II). Electron transmission micrographs (TEM) of the amphisomes (treated with OsO_4) revealed the presence of unilamellar vesicles of apparent diameter 760 Å. Dynamic light-scattering on a similarly prepared suspension of **7** indicated the presence of organizates having hydrodynamic diameters of 1200 Å. As above, TEM confirmed

(8) Medina, J. C.; Gay, I.; Chen, Z.; Echegoyen, L.; Gokel, G. W. *J. Am. Chem. Soc.* **1991**, *113*, 365.

(9) (a) Echegoyen, L. E.; Hernandez, J. C.; Kaifer, A.; Gokel, G. W.; Echegoyen, L. *J. Chem. Soc., Chem. Commun.* **1988**, 836. (b) Echegoyen, L. E.; Portugal, L.; Miller, S. R.; Hernandez, J. C.; Echegoyen, L.; Gokel, G. W. *Tetrahedron Lett.* **1988**, 4065. (c) Fasoli, H.; Echegoyen, L. E.; Hernandez, J. C.; Gokel, G. W.; Echegoyen, L. *J. Chem. Soc., Chem. Commun.* **1989**, 578. (d) Gokel, G. W.; Echegoyen, L. E. *Adv. Bioorg. Chem. Frontiers* **1990**, *1*, 116. (e) Muñoz, S.; Mallén, J. V.; Nakano, A.; Chen, Z.; Gay, I.; Echegoyen, L.; Gokel, G. W. *J. Chem. Soc., Chem. Commun.* **1992**, 520.

(10) Schultz, R. A.; White, B. D.; Dishong, D. M.; Arnold, K. A.; Gokel, G. W. *J. Am. Chem. Soc.* **1985**, *107*, 6659.

Table III. Debye Light-Scattering Profile for 2.19×10^{-3} M 1 in Water at 25 °C[a,b]

λ, nm	λ^{-2} ($\times 10^{-6}$)	turbidance[c] obsd	turbidance[c] calcd[d]	standard deviation	correlation coefficient
400	6.25	0.0881	0.0865	±0.001 25	0.9970
424	5.56	0.0775	0.0773		
450	4.94	0.0676	0.0691		
474	4.45	0.0610	0.0626		
500	4.00	0.0568	0.0566		
524	3.64	0.0515	0.0518		
550	3.30	0.0464	0.0473		
574	3.03	0.0457	0.0437		
600	2.78	0.0409	0.0404		
infinity			0.003 50[e]		

[a] Dispersed in water for 30 min, at 10 °C using a bath sonicator. [b] The typical vesicle diameter measured by dynamic light scattering is 200 ± 60 nm. [c] Addition of 50 mM sodium dodecyl sulfate lyses the vesicles and shows that the electronic absorption by the macrocyclic polyether headgroup is negligible at λ ≥ 400 nm. [d] The abbreviation "calcd turbidance" is that estimated according to a linear least-squares simulation of the data. [e] Note that the extrapolated turbidance at 0.003 50 corresponds to 99.2% transmittance. Given the inherent (≈ 1%) uncertainty in the spectrophotometric method, the intercept is within experimental error of 100% transmittance or 0 absorbance.

the presence of spherical vesicles of apparent diameter 1180 Å.

Static Turbidimetry. Laser-light scattering represents a powerful method for characterizing a collection of scattering particles, but the instrumentation required to conduct these measurements is not always readily available. Fortunately, conventional turbidimetry can provide information about the shape, linear dimension, polydispersity, and refractive index of scattering particles.[11] When a beam of light interacts with a sample, the light is attenuated by scattering according to the Beer–Lambert relationship (turbidance = $\log I_0/I = \tau \cdot \ell$), in which I_0 represents the intensity of the incident radiation, while I corresponds to the intensity of the unscattered light; τ stands for the turbidity of the medium, and ℓ represents the optical path across the analyte. The turbidity or extinction coefficient τ is defined by the expression $\tau = N \cdot Q_{sca}$, where N is the number of scattering particles per unit volume and Q_{sca} is the fraction of the incident radiant energy that is scattered in all directions.

The extinction efficiency Q_{sca}, and hence the turbidity, is determined by the radial dimension, the wavelength of irradiation, and the refractive index of the scattering particle relative to that of the medium. There are three types of radiating dipoles: Rayleigh scatterers (linear dimension much smaller than λ_0, any refractive index value), Debye scatterers (linear dimension $\approx \lambda_0$, refractive index near that of the medium), and Mie scatterers (linear dimension and refractive index both large). The extinction efficiency of a Debye radiator is given by the expression $Q_{sca} = 8\pi r^2(m-1)^2/\lambda^2$, in which r is the radius of the sphere, λ is the wavelength of the exciting radiation, and m is the relative refractive index, i.e., the ratio between the refractive indices of analyte and medium.[11] A plot of the turbidance of a spherical Debye scatterer vs. $1/\lambda^2$ is a straight line having a 0 intercept. Oster[11] has shown that the turbidance of rodlike or prolate ellipsoidal Debye oscillators varies linearly with $1/\lambda^3$. Debye scattering thus permits the distinction between the shapes—spherical or rodlike—of colloidal assemblies.

Data for static turbidimetry are presented in Table III for a suspension of 1 that has been dispersed in water at 2.19×10^{-3} M by mild ultrasonic irradiation in an immersion or bath sonicator. In the range between 600 and 400 nm, the turbidance varies from ≈0.0400–0.0900 and correlates linearly with $1/\lambda^2$. Extrapolation of the data to infinite wavelength gives an intercept of ≈0.003 50 (essentially 0 turbidance).

The light-scattering profile of 7 (dispersed in H_2O at 2.00 mM by mild ultrasonic irradiation) is shown in Table IV. The turbidance correlates linearly with $1/\lambda^2$ in the range 600–420 nm. Extrapolation to infinite wavelength gives an approximately 0 (–0.002 96) intercept. Taken together, these observations confirm that the bolyte vesicles behave as Debye scatterers.

Table IV. Debye Light-Scattering Profile of 2.00×10^{-3} M 7 in Water at 25 °C[a]

λ, nm	λ^{-2} (10^{-6})	turbidance[b] obsd	turbidance[b] cald[c]	standard deviation	correlation coefficient
424	5.56	0.104	0.0984	±0.003 29	0.9830
450	4.94	0.0847	0.0871		
474	4.45	0.0745	0.0781		
500	4.00	0.067	0.0699		
524	3.64	0.0620	0.0634		
550	3.30	0.0565	0.0572		
574	3.03	0.0547	0.0522		
600	2.78	0.0507	0.0477		
infinity			–0.002 96		

[a] Dispersed in water for 30 min at 10 °C, using a bath sonicator. [b] Electronic absorption by the macrocyclic polyether headgroup is negligible in the wavelength range indicated. [c] The abbreviation "calcd turbidance" is that estimated according to a linear least-squares simulation of the data.

Table V. Influence of Isotonic Dilution on the Aggregation State of 1 Measured by Dynamic Light Scattering in Water at 25 °C[a]

dilution	diameter, nm: unimodal distribution	cumulant distribution: by intensity	cumulant distribution: by weight
none	196 ± 62	214 ± 55	201 ± 65
4-fold	204 ± 48	226 ± 58	219 ± 70
8-fold	197 ± 57	215 ± 66	201 ± 74
16-fold	197 ± 58	208 ± 39	194 ± 46

[a] 10 mM bolyte, dispersed in water for 30 min at 10 °C, using a bath sonicator.

Scheme II

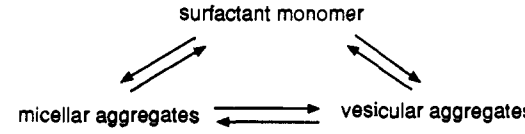

The Debye light-scattering profiles illustrate several properties of the bolyte vesicles: (1) their linear dimension is large, comparable to the wavelength of the incident radiation; (2) their shape is spherical rather than rodlike or prolate ellipsoidal; and most importantly, (3) their refractive index is small, similar to that of the aqueous medium. The size of vesicles from 1 (hydrodynamic diameter 200 ± 60 nm) is consistent with their preparation (by mild ultrasonic irradiation). Their spherical shape is confirmed by TEM. The near 1 relative refractive index probably results from the low hydrocarbon density inside the ultrathin hydrophobic matrix making them nearly optically transparent.

Bola-amphiphile monomers may fold about the center of their hydrocarbon backbone. In this conformation, surfactant bola-amphiphiles would aggregate preferentially as micelles in which the hydrophilic headgroups of each monomer are in contact with the bulk aqueous phase. Thus, the question arises of the possible dynamic equilibrium between micellar and vesicular pseudophases. The experiments discussed below were designed to address this possibility.

Effect of Isotonic Dilution. A typical micelle–vesicle equilibrium might be described as shown in Scheme II.[12] Dilution below the surfactant critical micelle concentration (cmc) shifts the equilibrium from aggregate to monomer. If micelles and vesicles coexist in dynamic equilibrium, deaggregation of the former results in vesicle lysis. The effect of serial isotonic dilution on the hydrodynamic size of a suspension of vesicles (mild sonication of

(11) Oster, G. Light Scattering. In *Physical Methods of Organic Chemistry*; A. Weissberger, A., Rossiter, B. W., Eds.; Wiley: New York, 1972; Vol. 1, Part IIIA.

(12) Miller, D. D.; Magid, L. J.; Evans, D. F. *J. Phys. Chem.* **1990**, *94*, 5421.

Table VI. Influence of Temperature on the Aggregation State of 1 Measured by Dynamic Light Scattering[a]

t, °C	unimodal diameter, nm
10	204 ± 67
20	196 ± 62
30	254 ± 47
35	700[c]
20	1110 ± 310

[a] 10 mM bolyte, dispersed in water for 30 min at 10 °C, using a bath sonicator. [b] The analyte is allowed to equilibrate thermally with the surroundings in the sample compartment for about 45 min before the turbidimetric profile is recorded. [c] Broad size distribution.

10 mM 1, deionized H_2O) is shown in Table V. In the undiluted suspension, analysis of the kinetic decay of the scattered intensity according to a single exponential term yields the unimodal hydrodynamic diameter of about 196 ± 62 nm. The cumulant method (scattered intensity is analyzed according to a multiexponential superposition) yields essentially the same value: 201 ± 65 nm. The suspension of vesicles is therefore homogeneous or radially monodisperse.

Upon 4-fold isotonic dilution (H_2O), the hydrodynamic diameter is found to be 204 ± 48 nm, which is the same (196 ± 62 nm) as found for the undiluted suspension. The same hydrodynamic diameter was found for 8-fold (197 ± 57 nm) and 16-fold (197 ± 58 nm) isotonic dilution. The insensitivity of vesicle size to dilution suggests that micellar and vesicular aggregates do not coexist simultaneously in this system. Note, however, that the inherently low turbidance of the analyte precludes further isotonic dilution experiments.

Effect of Temperature. Cooling an aqueous suspension of vesicles prepared from 15-crown-5 bola-amphiphile (1) from 20 to 10 °C had no effect on the hydrodynamic diameters (Table VI) which were within experimental error of each other at 196 ± 62 and 204 ± 67 nm, respectively. At 30 °C the diameter is still within the same error range at 254 ± 67 nm. However, heating to 35 °C led to increases in the scattered light intensity and in vesicle diameter (to about 700 nm). On cooling to 20 °C, the increased turbidence remained: laser-light scattering showed that the vesicles had grown to about 1000 nm in diameter (1 μm). Since the size growth observed at 35 °C was irreversible, it cannot be attributed to the opalescence point but indicates the onset of intervesicular fusion and the formation of large, multilamellar organizates.

Effect of Temperature in Acidic Media. Because of the unusual conditions in which archaebacteria survive, we were particularly interested in the temperature effect at low pH. Evans and collaborators[12] have demonstrated that as the temperature increases, thermal motion of the vesicular counterions increases and the surfactant headgroups dissociate to a greater extent. As the counterions dissociate, their ability to share charge or polarity present on the hydrophilic headgroups diminishes. This enhances local curvature along the vesicle surface and decreases aggregate size, eventually lysing them (→ micellar assemblies).[12] Above 25 °C, the cmc of charged surfactants normally increases with rising temperature,[13,14] so the concentration of free surfactant tends to increase with temperature. At sufficiently high temperatures, the magnitude of the cmc may become the same as the total surfactant concentration. In such a case, the monomer concentration would not exceed the cmc and no aggregate would form; the only species in solution will be the free surfactant monomer. The crown-derived bola-amphiphiles bear neutral, polar macrocycles that can be readily protonated to form charged headgroups.

As shown in Table VII, vesicles formed from 1 (10 mM, H_2O, pH 2) remain stable and monodisperse in the temperature range 23–40 °C. The hydrodynamic diameters vary as follows: 23 °C, 205 ± 57 nm; 35 °C, 244 ± 59 nm; 40 °C, 218 ± 70 nm. The vesicles retain their integrity at temperatures above 40 °C, although their size distribution broadens. Thus, a binary exponential superposition is needed in order to simulate the decay of the autocorrelation function: at 50 °C the component diameters and frequencies are 54 (89%) and 294 (11%) nm. At 60 °C, two component diameters are found: 106 (72%) and 360 (28%) nm. Even at 65 °C, the decay of the autocorrelation function remains binary: the component diameters are 169 and 300 nm and their frequencies are 77 and 23%.

Table VII. Influence of Temperature on the Aggregation State of 1 at pH = 2, Measured by Dynamic Light Scattering[a]

t, °C	unimodal diam, nm	cumulant distribution by weight			
		D_1, nm	%	D_2, nm	%
23	205 ± 57	202 ± 100	100		
35	244 ± 59	238 ± 45	100		
40	218 ± 70	206 ± 41	100		
50		54	89	294	11
60		106	72	360	28
65		169	77	300	23

[a] 10 mM bolyte, dispersed in water for 30 min at 10 °C using a bath sonicator. Thereafter, into a 2.00-mL aliquot of the vesicle suspension is added 20 μL of 1 M HCl to adjust the pH to 2. Upon mixing, the analyte is allowed to stand at ambient temperature for 1 h and subsequently is placed in the sample compartment to equilibrate thermally with the surroundings for 45 min before its light-scattering profile is recorded.

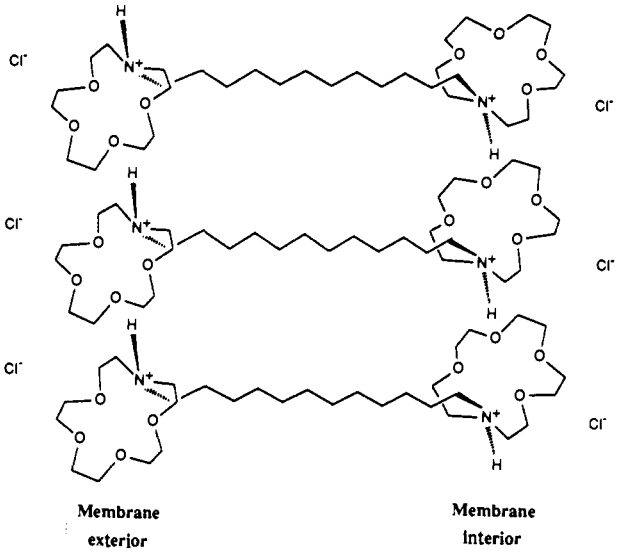

Figure 3. Possible structure for cooperative intermonomeric hydrogen-bridge formation along the exo- and endovesicular surfaces of 1 bola-amphisomes at pH 2.

The hydrodynamic size of the vesicles in the range 23–40 °C at pH 2 is the same (200 ± 60 nm) as measured in H_2O at ambient temperature. Thus, protonation of the azamacrocyclic headgroups does not cause electrostatic repulsions that would normally lead to an increase in vesicle diameter. In the range 40–65 °C, notwithstanding the broad radial distribution, the vesicles do not deaggregate. Strong ion-pairing interactions along the endo- and exovesicular surfaces must shield a substantial fraction of the electrostatic charge on the cationic headgroups, reducing intermonomeric repulsions and thus thermolysis. In this temperature range, the endo- and exovesicular surfaces are nearly neutral.

In the absence of a strong electrostatic barrier, electrically neutral amphisomes coalesce readily to yield large multilamellar assemblies. The data in Table VII fail to show the characteristic, spontaneous, monotonic growth in the vesicular diameter with increasing temperature. It is possible that a cooperative intermonomeric hydrogen-bonded network forms that inhibits both vertical and lateral diffusion of surfactant monomers, precluding vesicle coalescence.

Hydrogen-Bonded Domain Formation. In acidic media (e.g., pH 2), each surfactant headgroup in the bola-amphisome may

(13) Rosen, M. *Surfactants and Interfacial Phenomena*; Wiley: New York, 1978.
(14) Evans, D. D.; Wightman, P. J. *J. Colloid Interfac. Sci.* **1982**, *86*, 515.

adopt the conformation illustrated in Figure 3, whereby its acidic hydrogen atom is directed toward the macrocyclic polyether cavity of an adjacent headgroup. Consequently, a single intermonomeric hydrogen bridge triggers the synchronous, or cooperative, formation of endo- and exovesicular domains.

In order to attain their minimum potential energy, the bola-amphiphilic vesicles presumably maximize the total number of hydrogen bonds along their surfaces and simultaneously minimize unfavorable electrostatic repulsions. The latter condition is implemented by minimizing the charge density along both surfaces by maintaining strong pairing interactions between the cationic headgroups and their counterions. Although the endo- and exovesicular surfaces are nearly electrically neutral, as pointed out in the preceding section, the presence of hydrogen-bridged networks precludes fusion events by inhibiting both vertical diffusion (and thus intervesicular exchange of surfactant monomers) and transient lateral dissociation of the membrane, by which vesicles may rupture and subsequently reform to yield larger, heterogeneous, multilamellar organizates.[4]

Since each surfactant monomer forms a single hydrogen bond, the thermicity of domain formation may be estimated provided that the aggregation number, or the number of surfactant molecules incorporated into each vesicle, is known. The aggregation number of vesicles is typically large, between 10^5 and 10^6. Using 10^5 as a representative aggregation number for a monolayer vesicle, at least 2×10^5 hydrogen-bonding events will take place including both the external and internal surfaces. Using 2 kcal/mol as a working estimate for the enthalpy of hydrogen bond formation ($\approx 3.32 \times 10^{-24}$ kcal per bridge), it follows that domain formation releases energy to the extent of 400 cal/μmol of vesicles, an appreciable thermicity.

Conclusion

We have presented a novel family of bis(crown) bola-amphiphiles that aggregate into a previously unknown type of bola-amphisome. Both micelles and vesicles are formed by compounds in this family. The latter seem to predominate when the hydrocarbon spacer chains remain extended. The bola-amphisomes that derive from **1** and **7** are spherical and nearly optically transparent; their inherently low turbidity is caused by the low relative refractive index of the ultrathin monolayer membrane. Such transparent macromolecular aggregates may be useful as matrices in applications that require optically clear paths. These bola-amphisomes appear to be stabilized by the formation of intermonomeric endo- and exovesicular hydrogen-bonded domains in acidic media. Fendler[15] stabilized surfactant vesicles against fusion by photoinduced covalent polymerization of their corresponding headgroups, a process that may not be required in the present systems. The vesicles reported here, like those in the membrane of thermoacidophilic archaebacteria, may enjoy unusual strength even under severe conditions.

Experimental Section

^{1}H-NMR spectra were recorded on a Varian XR-400 NMR Spectrometer or on a Hitachi Perkin-Elmer R-600 high-resolution NMR spectrometer for samples in $CDCl_3$ solvents and are reported in ppm (δ) downfield from internal $(CH_3)_4Si$. ^{13}C-NMR spectra were recorded on a JEOL FX90Q or Varian XL-400 NMR spectrometer or as noted above. Infrared spectra were recorded on a Perkin-Elmer 1310 infrared spectrophotometer and were calibrated against the 1601 cm^{-1} band of polystyrene. Melting points were determined on a Thomas-Hoover apparatus in open capillaries and are uncorrected. Thin-layer chromatographic (TLC) analyses were performed on aluminum oxide 60 F-254 neutral (Type E) with a 0.2-mm layer thickness or on silica gel 60 F-254 with a 0.2-mm layer thickness. Preparative chromatography columns were packed with activated aluminum oxide (MCB 80-325 mesh, chromatographic grade, AX 611) or with kieselgel 60 (70-230 mesh). Chromatotron chromatography was performed on a Harrison Research Model 7924 Chromatotron with 2-mm-thick circular plates prepared from kieselgel 60 PF-254. All reactions were conducted under dry N_2 unless otherwise noted. All reagents were of the best grade commercially available and were distilled, recrystallized, or used without further purification, as appropriate. Molecular distillation temperatures refer to the oven temperature of a Kugelrohr apparatus. Combustion analyses were performed by Atlantic Microlab, Inc., Atlanta, GA, and are reported as percents.

General Procedure for the Preparation of Diacyl Bola-Amphiphiles (A). A solution of the corresponding alkyldiacid (2 mmol) in $SOCl_2$ (1 mL) was stirred and heated to reflux for 12 h. The excess $SOCl_2$ was removed by azeotropic distillation of toluene (3 × 10 mL). To a vigorously stirred solution of the azacrown (3.8 mmol) and triethylamine (4 mmol) in benzene (50 mL) was added a solution of the acyl chloride in benzene (50 mmol). The temperature of the reaction was kept at 0–5 °C during the addition and then stirred at room temperature for 48 h. The salts were filtered and washed with CH_2Cl_2 (3 × 15 mL). The solvent was evaporated, and the residue was taken up by CH_2Cl_2 (50 mL) and washed with 3 N HCl (3 × 10 mL), saturated Na_2CO_3 (2 × 10 mL), and H_2O (2 × 15 mL). The organic layer was dried and evaporated in vacuo, and the resulting oil was purified by column chromatography on alumina and/or recrystallization from the appropriate solvent mixtures to afford the acylated bolytes **6–10** in yields ranging from 58 to 79%.

General Procedure for the Reduction of Diacyl Bolytes (B). A vigorously stirred solution containing the acylated bolyte (0.2 mmol) and $LiAlH_4$ (152 mg, 4 mmol) in THF (50 mL) was heated under reflux for 24 h. Calcium chloride drying tubes were used to maintain a dry atmosphere. The excess of hydride was destroyed with a mixture of THF–H_2O (80:20 v/v). The alumina formed was filtered off, and the filtrate was evaporated to dryness. The residual oil was purified by column chromatography on alumina and/or recrystallization from the adequate solvent mixtures to afford the bola-amphiphiles in yields ranging from 70 to 78%.

***N*-[12-(Aza-15-crown-5)dodecyl]aza-15-crown-5 (1).** *N*-[12-(Aza-15-crown-5)(1,12-dodecanedioyl)]aza-15-crown-5 (precursor to **1**) was prepared according to method A from aza-15-crown-5 (1.5 g, 6.84 mmol) and 1,12-dodecanedioyl chloride (913 mg, 3.42 mmol). The product was purified by column chromatography (alumina, 0–2% MeOH/CH_2Cl_2) and was isolated as a pale yellow oil (1.53 g, 71%). ^{1}H NMR: 1.20–1.86 (br s, 16 H), 2.32 (m, 4 H), 3.62–3.84 (m, 40 H). IR (neat): 2910 (s), 1645 (s), 1480, 1420, 1130 (s), 1080 cm^{-1}.

N-[12-(Aza-15-crown-5)dodecyl]aza-15-crown-5 (**1**) was obtained by reduction of the diamide (see above, 1.00 g, 1.58 mmol) with $LiAlH_4$ (840 mg, 22.1 mmol) according to Method B. The resulting oil was purified by column chromatography (alumina, 2–10% i-PrOH/hexanes and then 0–2% MeOH/CH_2Cl_2) to afford the product as a thick yellow oil (0.73 g, 76%). ^{1}H NMR ($CDCl_3$): 1.16–1.74 (br s, 20 H), 2.3–2.5 (m, 4 H) 2.78 (t, 8 H), 3.52–3.78 (m, 32 H). IR (neat): 2920 (s), 2880, 1460 (s), 1350, 1290, 1080 (s), 970 cm^{-1}. Anal. Calcd for $C_{32}H_{64}N_2O_8$: C, 63.52; H, 10.67. Found: C, 63.15; H, 10.38.

***N*-[16-(Aza-15-crown-5)hexadecyl]aza-15-crown-5 (2).** *N*-[16-(Aza-15-crown-5)(1,16-hexadecanedioyl)]aza-15-crown-5 (precursor to **2**) was prepared according to method A from aza-15-crown-5 (1.5 g, 6.85 mmol) and 1,16-hexadecanedioyl chloride (1.16 g, 3.6 mmol). The product was purified by column chromatography (alumina, 0–2% MeOH/CH_2Cl_2) and was isolated as a colorless oil that crystallized upon standing (1.65 g, 68%), mp 72–73 °C. ^{1}H NMR: 1.26–1.88 (br, 24 H), 2.28 (m, 4 H), 3.58–3.82 (m, 40 H). IR (KBr): 2960 (s), 1640 (s), 1480, 1420, 1310, 1260, 1070 (s), 1000, 960 cm^{-1}.

N-[16-(Aza-15-crown-5)hexadecyl]aza-15-crown-5 (**2**) was obtained from the compound described above (0.8 g, 1.16 mmol) and $LiAlH_4$ (882 g, 23.2 mmol). The residual oil was purified by column chromatography (alumina, 0–1% MeOH/CH_2Cl_2), followed by recrystallization (EtOAc) to afford the product as a white solid (0.68 g, 78%), mp 65–66 °C. ^{1}H NMR: 1.18–1.78 (br s, 28 H), 2.3–2.48 (m, 4 H) 2.78 (t, 8 H), 3.52–3.80 (m, 32 H). IR (KBr): 2920 (s), 2890, 1470(s), 1320, 1290, 1070(s), 1010, 990 cm^{-1}. Anal. Calcd for $C_{36}H_{72}N_2O_8$: C, 65.38; H, 10.98. Found: C, 65.10; H, 10.61.

***N*-[1,22-Bis(*N*-aza-15-crown-5)docosane Diamide (3).** The title compound was prepared according to method A from aza-15-crown-5 (1.50 g, 6.85 mmol) and docosanedioyl dichloride (1.52 g, 4 mmol). The product was purified by column chromatography (alumina, 0–1% CH_3OH/CH_2Cl_2), followed by recrystallization (EtOAc) to afford **3** as a white solid (2.25 g, 69%), mp 76–78 °C. ^{1}H NMR: 1.18–1.78 (br s, 36 H), 2.24 (m, 4 H), 3.48–3.78 (m, 40 H). IR (KBr): 2960 (s), 1640 (s), 1490, 1440, 1260, 1050 (s), 970 cm^{-1}. Anal. Calcd for $C_{42}H_{80}N_2O_{10}$: C, 65.23; H, 10.43. Found: C, 65.51; H, 10.66.

***N*-[22-(Aza-15-crown-5)docosanyl]aza-15-crown-5 (4).** The title compound was obtained by reduction of the corresponding bis(bola-amphiphile) (1.09 g, 1.29 mmol) in the presence of $LiAlH_4$ (912 mg, 24 mmol) according to method B. The product was purified by column chromatography (alumina, 0–2% *i*-PrOH/hexanes, and then 0–2% CH_3OH/CH_2Cl_2), followed by crystallization from EtOAc/hexanes (4:1

(15) Fendler, J. H. *Isr. J. Chem.* **1985**, *25*, 3.

v/v) to yield the product (0.71 g, 73%) as a white solid, mp 55–56 °C. ^{1}H NMR: 1.20–1.78 (br s, 40 H), 2.32–2.46 (m, 4 H), 2.78 (t, 8 H), 3.48–3.82 (m, 48 H). IR (KBr): 2920 (s) 2880, 1460 (s), 1300, 1250, 1080 (s) 980 cm^{-1}. Anal. Calcd for $C_{42}H_{84}N_2O_8$: C, 67.68; H, 11.37. Found: C, 67.45; H, 11.04.

***N*-[10-(Aza-18-crown-6)decyl]aza-18-crown-6 (5).** The title compound was prepared from aza-18-crown-6 (1.12 g, 4.24 mmol), 1,10-decaneditosylate (1.02 g, 2.12 mmol), and Na_2CO_3 (4.49 g, 42.4 mmol) as described above. Column chromatography (alumina, 0.2% MeOH/CH_2Cl_2) affords the product as a pale yellow oil (0.63 g, 45%). ^{1}H NMR: 1.1–1.8 (br s, 16 H), 2.5–3.8 (m, 52 H). IR (neat): 2940 (s), 1610, 1470, 1320, 1250, 1100 cm^{-1}. Anal. Calcd for $C_{34}H_{68}N_2O_{10}$: C, 61.45; H, 10.24. Found: C, 61.24; H, 10.43.

***N*-[12-(Aza-18-crown-6)(1,12-dodecanedioyl)]aza-18-crown-6 (6).** This compound was prepared according to method A from aza-18-crown-6 (2.28 g, 8.68 mmol) and 1,12-dodecanedioyl chloride (4.4 mmol). The resulting oil was purified by column chromatography (alumina, 5–10% *i*-PrOH/hexanes, and then 0–1% MeOH/CH_2Cl_2) to afford **6** as a pale yellow oil (2.47 g, 79%). Anal. Calcd for $C_{36}H_{68}N_2O_{12}$: C, 59.95; H, 9.51. Found: C, 59.62; H, 9.82.

***N*-[12-(Aza-18-crown-6)dodecyl]aza-18-crown-6 (7).** This compound was obtained from **6** (1.72 g, 2.39 mmol) and $LiAlH_4$ (1.82 g, 47.9 mmol) according to the general method B. Purification involved column chromatography (alumina, 0–5% *i*-PrOH/hexanes, and then 0–2% MeOH/CH_2Cl_2) to afford the bola-amphiphile as a thick yellow oil (1.19 g, 72%). ^{1}H NMR: 1.14–1.68 (br s, 20 H), 2.3–2.52 (m, 4 H), 2.76 (t, 8 H) 3.48–3.76 (m, 40 H). IR (neat): 2910 (s), 2890, 1460(s), 1340, 1280, 1080 (s), 980 cm^{-1}. Anal. Calcd for $C_{36}H_{72}N_2O_{10}$: C, 62.38; H, 10.48. Found: C, 62.10; H, 10.21.

***N*-[16-(Aza-18-crown-6)(1,16-hexadecanedioyl)]aza-18-crown-6 (8).** The title compound was prepared according to method A from aza-18-crown-6 (2.0 g, 7.6 mmol) and 1,16-hexadecanedioyl dichloride (1.29 g, 4 mmol). The resulting oil was purified by column chromatography (alumina, 0–2% CH_3OH/CH_2Cl_2) to afford the product as a thick, colorless oil (2.17 g, 72%). ^{1}H NMR: 1.22–1.81 (br s, 24 H), 2.32 (m, 4 H), 3.58–3.82 (m, 48 H). IR (neat): 2970 (s), 1645 (s), 1470, 1420, 1320, 1060 (s), 980 cm^{-1}. Anal. Calcd for $C_{40}H_{76}N_2O_{12}$: C, 61.81; H, 9.86. Found: C, 61.49; H, 9.63.

***N*-[16-(Aza-18-crown-6)hexadecyl]aza-18-crown-6 (9).** *N*-[16-(Aza-18-crown-6)(1,16-hexadecanedioyl]aza-18-crown-6 (precursor to **9**) was prepared according to method A from aza-18-crown-6 (2.0 g, 7.6 mmol) and 1,16-hexadecanedioyl chloride (4 mmol). The resulting oil was purified by column chromatography (alumina, 0–2% MeOH/CH_2Cl_2) to afford the product as a thick colorless oil (2.17 g, 72%). ^{1}H NMR ($CDCl_3$): 1.22–1.81 (br s, 24 H), 2.32 (m, 4 H), 3.58–3.82 (m, 48 H). IR (crude): 2979 (s), 1645 (s), 1470, 1420, 1320, 1060 (s), 980 cm^{-1}.

***N*-[16-(Aza-18-crown-6)hexadecyl]aza-18-crown-6 (9).** This compound was obtained from the diamide described above (1 g, 1.28 mmol) and $LiAlH_4$ (973 mg, 25.6 mmol) according to method B. The resulting oil was purified by column chromatography (0–1% MeOH/CH_2Cl_2) to afford the product as a waxy solid upon standing (0.69 g, 70%). ^{1}H NMR: 1.16–1.72 (br s, 28 H), 2.32–2.46 (m, 4 H), 2.78 (t, 8 H), 3.50–3.78 (m, 40 H). IR (KBr): 2910 (s), 2890, 1480 (s), 1320, 1280, 1070, 990 cm^{-1}. Anal. Calcd for $C_{40}H_{80}N_2O_{10}$: C, 64.12; H, 10.77. Found: C, 64.28; H, 10.58.

***N*-[22-(Aza-18-crown-6)docosanyl]aza-18-crown-6 (10).** *N*-[22-(Aza-18-crown-6)(1,22-docosanedioyl]aza-18-crown-6 was prepared according to method A from aza-18-crown-6 (2 g, 7.604 mmol) and docosanedioyl chloride (4 mmol). The product was purified by column chromatography (alumina, 0–1% MeOH/CH_2Cl_2), followed by recrystallization (EtOAc) to afford the product as a white solid (1.93 g, 58%), mp 49–51 °C. ^{1}H NMR: 1.24–1.88 (br s, 36 H), 2.28 (m, 4 H), 2.52–3.80 (m, 48 H). IR (KBr): 2980 (s), 1640 (s), 1480, 1440, 1300, 1280, 1060 (s), 980 cm^{-1}.

N-[22-(Aza-18-crown-6)docosanyl]aza-18-crown-6 (**10**) was obtained by reduction of (1 g, 1.17 mmol) in the presence of $LiAlH_4$ (889 mg, 23.4 mmol) according to the general method B. The product was purified by column chromatography (alumina, 1–5% i-PrOH/hexanes, and then 0–1% MeOH/CH_2Cl_2), followed by recrystallization from EtOAc/hexanes (4:1 v/v) to yield the bola-amphiphile as a white solid (0.72 g, 71%), mp 58–59 °C. ^{1}H NMR: 1.18–1.80 (br s, 40 H) 2.34–2.48 (m, 4 H), 2.76 (t, 8 H), 3.52–3.80 (m, 40 H). IR (KBr): 920 (s), 2890, 1470 (s), 1300, 1270, 1080 (s), 990 cm^{-1}. Anal. Calcd for $C_{46}H_{92}N_2O_{10}$: C, 66.28; H, 11.13. Found: C, 65.91; H, 10.96.

Preparation of Bis(*N*-dodecylaza-18-crown-6) Ether (11). 12-Formatododecanoic Acid, A. In a 100-mL round-bottomed flask, 12-hydroxydodecanoic acid (2 g, 9.25 mmol) and 50 mL of formic acid (85%) were stirred to reflux for 4 h. The reaction mixture was allowed to cool, and 100 mL of H_2O was added. The solution was filtered on the pump, and the resulting residue was dissolved in CH_2Cl_2 (20 mL) and filtered through an alumina bed to afford the product as a white solid (2.1 g, 91%), mp 61–62 °C. IR (KBr): 2920 (s), 1740 (s), 1450, 1190(s), 900 cm^{-1}. ^{1}H NMR: 1.1–1.80 (m, 18 H), 2.10–2.40 (m, 2 H), 4.05–4.35 (m, 2 H), 8.06 (s, 1 H).

***N*-(Hydroxydodecanoyl)aza-18-crown-6, B.** A solution of **A** (976 mg, 4 mmol) in $SOCl_2$ (3.81 g, 32 mmol) was stirred and heated to reflux for 12 h. The excess $SOCl_2$ was removed by azeotropic distillation of toluene (3 × 10 mL), and the product was dissolved in benzene (50 mL) and added dropwise to a vigorously stirred solution of aza-18-crown-6 (1.0 g, 3.8 mmol) and triethylamine (1.01 g, 10 mmol) in benzene (50 mL). The temperature of the reaction was kept at 0–5 °C during the addition and then stirred at room temperature for 24 h, followed by a refluxing period of 4 h. After the reaction was completed the salts were filtered and washed with CH_2Cl_2 (3 × 15 mL), the solvent was evaporated, and the residue was taken up by CH_2Cl_2 (100 mL). The formate ester was hydrolyzed with 50 mL of 10% NaOH in methanol by stirring for 10 min at room temperature. Water (20 mL) was then added, and the phases were separated. The organic layer was then washed with 3 N HCl (3 × 10 mL) saturated Na_2CO_3 (2 × 10 mL), and H_2O (2 × 15 mL). The organic layer was dried and evaporated in vacuo, and the residue was purified by column chromatography (alumina, 0–3% MeOH/CH_2Cl_2) to afford the product as a pale yellow oil (1.24 g, 71%) that solidified upon refrigeration (mp 26–27 °C). IR (neat): 3560 (s), 2980 (s), 1640 (s), 1470 (s), 1380 (s), 1310, 1150 (s), 920 cm^{-1}. ^{1}H NMR: 1.05–1.92 (br s, 18 H), 2.18–2.45 (m, 3 H), 3.45–3.80 (br s, 26 H).

Bis(N-dodecanedioylaza-18-crown-6) Ether, C. To a vigorously stirred solution of **B** (0.45 g, 0.98 mmol) and NaH (95 mg, 4 mmol) in dry THF (20 mL) was added *N*-bromododecanoylaza-18-crown-6 (550 mg, 1.05 mmol), and the mixture was refluxed under N_2 for 48 h. The reaction was cooled to room temperature and quenched with a mixture of THF/H_2O (80:20 v/v) (20 mL). The salts were filtered off, and the filtrate was evaporated in vacuo. The residue was dissolved in CH_2Cl_2 (50 mL), washed with H_2O (3 × 10 mL), and dried ($MgSO_4$). The solvent was evaporated, and the residue was purified by column chromatography (3% deactivated alumina, 0.5–1% i-PrOH/CH_2Cl_2) to afford the product as a pale yellow oil (0.42 g, 48%) IR (neat): 1280 (s), 1630 (s), 1480 (s), 1370, 1300, 1110 (s), 910 cm^{-1}. ^{1}H NMR: 1.12–1.80 (br s, 36 H), 2.15–2.40 (m, 4 H), 3.40–3.78 (m, 52 H).

Bis(*N*-dodecylaza-18-crown-6) Ether (11). A vigorously stirred solution containing the bolyte C (0.22 g, 0.243 mmol) and $LiAlH_4$ (0.13 g, 3.4 mmol) in THF (40 mL) was heated to reflux for 24 h under a dry N_2 atmosphere. The excess of hydride was destroyed with a mixture of THF/H_2O (80:20 v/v). The alumina formed was filtered off, and the filtrate was evaporated to dryness. The residue was purified by column chromatography (3% deactivated alumina (0–1% i-PrOH/CH_2Cl_2) to afford the product as a pale yellow oil (0.13 g, 61%) IR (neat): 2910 (s), 2890, 1460 (s), 1350, 290, 1080 (s), 920 cm^{-1}. ^{1}H NMR: 1.05–1.7 (br s, 36 H), 1.8–2.1 (m, 4 H), 2.34–2.48 (m, 4 H), 2.74 (t, 8 H), 3.42–3.80 (m, 52 H). Anal. Calcd for $C_{48}H_{96}N_2O_{11}$: C, 65.70; H, 11.03. Found: C, 65.42; H, 11.21.

1,12-Dithia-(*N*-dodecanoylaza-18-crown-6)dodecane (12). To a vigorously stirred solution of 1,12-dodecanedithiol (61 mg, 0.26 mmol) and NaH (124 mg, 0.26 mmol) in dry THF (50 mL) was added *N*-(bromododecanoyl)aza-18-crown-6 (0.25 g, 0.52 mmol). The mixture was refluxed under N_2 for 4 days. The reaction was cooled to room temperature and quenched with a mixture of THF/H_2O (80:20 v/v, 50 mL). The salts were filtered off, and the filtrate was evaporated in vacuo. The residue was dissolved in CH_2Cl_2 (50 mL), washed with H_2O (3 × 10 mL), and dried ($MgSO_4$). The solvent was evaporated, and the residue was purified by column chromatography (alumina, 2–5% i-PrOH/hexanes, and then 0–1% MeOH/CH_2Cl_2) to afford the bolyte as a waxy solid upon standing (0.19 g, 57%). ^{1}H NMR: 1.18–1.82 (m, 48 H). IR (KBr): 2920 (s), 2890, 1470, 1350, 1280, 110 (s), 1000, 960 cm^{-1}. Anal. Calcd for $C_{60}H_{16}N_2O_{12}S_2$: C, 64.23; H, 10.43. Found: C, 64.48; H, 10.74.

Vesicle Preparation. The corresponding compounds were weighed out to make 2–5 mM suspensions in deionized water, which were then sonicated for 30 min at 10 °C using a Branson Cell Disruptor, Model 185, operated at 30 W. Afterwards, the suspensions were centrifuged for 10–15 min and filtered through Nucleopore polycarbonate membranes of 1-μm porosity.

Mild Ultrasonic Irradiation Method. Into a 50-mL round-bottom flask were placed 40 mg (6 μmol) of bola-amphiphile **1**, or alternatively **7**, followed by 7 mL of deionized water. After the flask and its contents were gently swirled, the bola-amphiphilic compound was readily suspended in the medium to give a hazy suspension, which became nearly optically transparent upon dispersion (30 min at 10 °C) by means of a Branson immersion or bath sonicator. Thereafter, the vesicle preparation was diluted 4-fold using deionized water to yield the final stock suspen-

sion that contained approximately 2 mM bolyte.

Static Turbidimetry. A 3.00-mL aliquot of the stock analyte containing the suspension of mildly sonicated vesicles was transferred into a quartz cuvette, and the turbidimetric profile at ambient temperature was recorded in the range between 400 and 600 nm, using a Hewlett-Packard Model 8452 A diode array spectrophotometer set with an integration time of 10 s. Deionized water was used as the reference in a cuvette that was matched with respect to that holding the analyte. *Note*: Because absorption spectrophotometers are not ideal turbidimeters, the corresponding turbidance measurements will vary somewhat according to the instrument that is employed.

Vesicle Lysis. After recording the turbidance spectrum, the organizates were disassembled by the addition of about 200 μL of 0.775 M sodium dodecyl sulfate into 3.00 mL of analyte, to give a final concentration of about 0.0500 M in SDS, which is well above the value of its critical micelle concentration of 8.16 mM in water. The electronic absorption spectrum of the clear solution was subsequently recorded in the range between 400 and 600 nm. Observe that the optical densities of the bolyte solutions measured thereby were negligible above 400 and 424 nm, respectively, in the case of bolytes **1** and **7**.

Dynamic Turbidimetry. Laser-light-scattering profiles were recorded by means of a Coulter Model N45D spectrometer equipped with a 632.8-nm helium-neon laser operated at 4 nW. In the case of the large mildly sonicated vesicles, a 2.00-mL aliquot of the suspension was placed in the sample compartment and then allowed to equilibrate thermally with the surroundings for 45 min before the light-scattering profile was recorded. The corresponding measurements of the hydrodynamic diameter as a function of increasing temperature were carried out in sequence using the same stoppered sample, which was thermostated with ±0.2 °C. In a representative experiment, the sample time was set at about 20 μs, the acquisition time was 500 s, and the scattering angle was fixed at 90°.

Transmission Electron Microscopy was also used to detect and measure the vesicles. The respective samples were prepared by fixing the aggregates with osmium tetroxide and then staining them with zinc uranyl acetate. Accordingly, fixation was carried out by adding 1 drop of 4% OsO_4 to 1 mL of the vesicle suspension; upon being allowed to stand at room temperature for 1 h, the mixture was stained with 2% (w/w) uranyl acetate. A drop of the suspension was then placed on a carbon-coated copper grid and blotted dry after 60 s. Finally, the sample was examined by means of a Phillips E.M. 300 electron microscope operated at 60 kV.

Acknowledgment. We thank the NIH for a grant (GM-36262) that supported portions of this work. In addition, S.M. was supported by a NIH Minority Post-doctoral Supplement, for which we are grateful.

Methanolysis of K-Region Arene Oxides: Comparison between Acid-Catalyzed and Methoxide Ion Addition Reactions

Nashaat T. Nashed,*,‡ Ad Bax,† Richard J. Loncharich,§,⊥ Jane M. Sayer,‡ and Donald M. Jerina‡

Contribution from the Laboratories of Bioorganic Chemistry and Chemical Physics, National Institute of Diabetes and Digestive and Kidney Diseases, and Molecular Graphics and Simulation Laboratory, Division of Computer Research and Technology, The National Institutes of Health, Bethesda, Maryland 20892. *Received June 8, 1992. Revised Manuscript Received October 5, 1992*

Abstract: Reactions of K-region arene oxides of benz[*a*]anthracene (BA-O) and its 1- (1-MBA-O), 4- (4-MBA-O), 7- (7-MBA-O), 11- (11-MBA-O), 12-methyl- (12-MBA-O), 7,12-dimethyl-(DMBA-O), and 7-bromo- (7-BrBA-O) substituted derivatives, benzo[a]pyrene (BaP-O), benzo[*c*]phenanthrene (BcP-O), benzo[*e*]pyrene (BeP-O), benzo[*g*]chrysene (BgC-O), chrysene (Chr-O), dibenz[*a,h*]anthracene (DBA-O), phenanthrene (Phe-O), 3-bromophenanthrene (3-BrPhe-O), and pyrene (Pyr-O) with acid and methoxide ion in methanol, are compared. For the acid-catalyzed reaction, products consist of *cis*- and *trans*-methanol adducts and phenols. There is no isotope effect on the ratio of phenols to solvent adducts produced from Phe-O or BcP-O when deuterium is substituted for the hydrogen that migrates. This observation is consistent with a mechanism in which product distribution in acid is determined by the relative rates of solvent capture and conformational inversion of a carbocation intermediate. As expected, only *trans*-methanol adducts, consisting of regioisomeric mixtures for unsymmetrical arene oxides, are formed from the reaction of methoxide ion with K-region arene oxides. The use of methanol permits the identification of products formed at each benzylic position of unsymmetrical arene oxides. Rate data for reactivity at each position could be fitted to the equation $\log k_{MeO}/k_{MeO}^{Phe\text{-}O} = m(\log k_H/k_H^{Phe\text{-}O}) + b$, where k_{MeO} and k_H are the second-order rate constants of the methoxide ion addition and acid-catalyzed reaction, respectively, and $k_{MeO}^{Phe\text{-}O}$ and $k_H^{Phe\text{-}O}$ are the corresponding rate constants for the reference compound phenanthrene oxide. A plot of $\log k_{MeO}/k_{MeO}^{Phe\text{-}O}$ vs $\log k_H/k_H^{Phe\text{-}O}$ for the reaction of 1-MBA-O, 12-MBA-O, DMBA-O, BcP-O, and BgC-O, which have either a methyl substituent in the bay region or a sterically crowded fjord region which affects the planarity of the molecules, defined one line ($m = 0.31 \pm 0.02$, $b = 0.67 \pm 0.09$), whereas a plot of the data for the reaction of the nearly planar arene oxides BA-O, 4-MBA-O, 7-MBA-O, 11-MBA-O, BaP-O, BeP-O, Chr-O, DBA-O, Phe-O, and Pyr-O defined a different line ($m = 0.33 \pm 0.07$, $b = -0.05 \pm 0.05$). The nonzero intercept for the sterically crowded, nonplanar arene oxides indicates a steric acceleration of their rates of methoxide ion addition. The positive slopes of both lines are consistent with an S_N2 mechanism with an unsymmetrical transition state in which the epoxide C–O bond breaking is more advanced than the formation of the new C–O bond to methoxide ion, such that a partial positive charge is developed on the aromatic moiety.

Introduction

Both benzo-ring and K-region arene oxides are common mammalian metabolites of the environmentally ubiquitous polycyclic aromatic hydrocarbons.[1a] These inherently cytotoxic and genotoxic metabolites are initially formed by the action of the cytochromes P450 and are subsequently transformed into *trans*-dihydrodiols and glutathione conjugates by microsomal xenobiotic epoxide hydrolase and the cytosolic glutathione *S*-transferases, respectively. In both cases, these enzymes display substantial enantio- and regioselectivity toward arene oxide substrates.[1-3] Detailed understanding of their mechanisms of

* Address correspondence to Dr. Nashaat T. Nashed, National Institutes of Health, Bldg. 8, Room 1A02, Bethesda, MD 20892, Tel. (301)-496-1780, Fax (301)-402-0008.

‡ Laboratory of Bioorganic Chemistry.

† Laboratory of Chemical Physics.

§ Molecular Graphics and Simulation Laboratory.

⊥ Current address: Supercomputer Applications and Molecular Design, Eli Lilly and Company, Lilly Corporate Center, Indianapolis, IN 46285-0403.

(1) (a) Boyd, D. R.; Jerina, D. M. In *Small Ring Heterocycles*; Hassner, A., Ed.; John Wiley and Sons, Inc.; New York, 1985; Vol. 42, Part 3, pp 197-282. (b) Armstrong, R. N. *Chem. Res. Toxicol.* **1991**, *4*, 131.

0002-7863/93/1515-1711$04.00/0